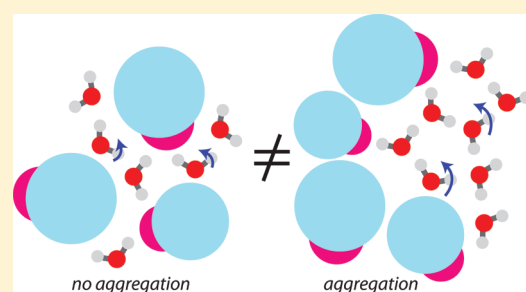


Dynamics of Water in Concentrated Solutions of Amphiphiles: Key Roles of Local Structure and Aggregation

Guillaume Stirnemann,[†] Fabio Sterpone,^{*,†,‡} and Damien Laage^{*}

Ecole Normale Supérieure, Chemistry Department, UMR CNRS-ENS-UPMC 8640, 24 rue Lhomond, 75005 Paris, France

ABSTRACT: Water translational and reorientational dynamics in concentrated solutions of amphiphiles are investigated through molecular dynamics simulations and analytic modeling. We evidence the critical importance of the solute concentration in determining the magnitude of the slowdown in water dynamics compared to the bulk situation. The comparison of concentrated aqueous solutions of tetramethylurea, which tends to aggregate, and of trimethylamine *N*-oxide, which does not, shows the dramatic impact of solute clustering on the water dynamics. No significant decoupling of the reorientation and translation dynamics of water is observed, even at very high solute concentrations. The respective roles of energetic and topological disorders in determining the translational subdiffusive water dynamics in these confining environments are discussed. The water reorientational dynamics is shown to be quantitatively described by an extended jump model which combines two factors determined by the local structure: the transition-state excluded volume and the transition-state hydrogen-bond strength.



1. INTRODUCTION

Water in confining environments has received increasing attention because of its relevance for a broad range of situations of importance in nature as well as in technology. In biology, water is found within ion channels and protein cavities.^{1–4} In geology, confinement occurs, for example, in mineral inclusions and between sheets of clay.⁵ In chemistry, confined water can be found, for example, within fuel-cell membranes⁶ and within reverse micelles.^{7–11} In engineering science, the recent development of nanotechnologies poses the problem of water behavior when confined at this scale, for example, in synthetic nanopores,¹² carbon nanotubes,¹³ Vycor glasses,¹⁴ and zeolites.¹⁵ Confinement leads to dramatic changes in the structure, dynamics, and thermodynamics of water compared to the bulk.^{2,16–19}

Very concentrated aqueous solutions can also act as a confining environment for water through a crowding effect.²⁰ One important example is the cell cytoplasm,² where a significant fraction of the space is occupied by macromolecules whose concentration can range up to 400 g·L⁻¹.^{2,21} The behavior of water in the cytoplasm is still much debated, especially in cells of extreme halophilic archaeon. While quasi-elastic neutron scattering (QENS) experiments²² find a dramatic 250-fold slowdown of the water dynamics in these cells, NMR reports²³ a more moderate, 15-fold slowdown. A possible but still speculative explanation may be the occurrence of a decoupling between the translational dynamics measured by QENS and the reorientational dynamics measured by NMR, induced by the high solute concentration and the confinement of water.

A recent series of experiments,^{24–28} mainly based on ultrafast infrared spectroscopy techniques, measured the dynamics of water in concentrated solutions of amphiphiles to investigate

hydrophobic hydration dynamics. These results were interpreted assuming that hydrophobic groups “immobilize” several water molecules, or at least induce a very large slowdown of their dynamics, and that this slowdown factor is concentration-independent.^{24–28} However, other studies, both theoretical²⁹ and experimental,^{30–32} suggest that the water slowdown is very sensitive to the concentration, for example for aqueous solutions of amphiphiles^{29,32} and of peptides,³¹ and that the water molecules are only very moderately retarded in dilute solutions.^{29,32–34} In addition, the ultrafast infrared studies employed solutions of amphiphiles beyond the aggregation threshold but did not address the potential effect of solute clustering on the water dynamics.^{24–28}

We combine here molecular dynamics simulations and analytic modeling to study water dynamics in solutions of amphiphiles of increasing concentration, focusing on the high concentration regime. To analyze the impact of aggregation on the dynamics of water, we have selected two amphiphiles with very different behaviors, tetramethylurea (TMU), which is experimentally known^{35–37} to readily aggregate at very low concentrations, and trimethylamine *N*-oxide (TMAO), which remains unaggregated up to very high concentrations³⁸ (Figure 1).

The outline of the remainder of this article is as follows: In section 2, we detail our molecular dynamics simulation methodology. In section 3 we first analyze the microscopic structure of the TMAO and TMU binary solutions, focusing on the different propensities of the two solutes to aggregate in water as

Received: December 17, 2010

Revised: February 10, 2011

Published: March 08, 2011

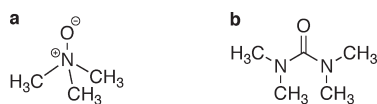


Figure 1. Chemical structures of (a) TMAO and (b) TMU.

concentration increases. In section 4, we then investigate the water translational and reorientational dynamics in these solutions of increasing concentration and show that water dynamics slows down dramatically with increasing solute concentration, and that the effect is more pronounced for TMAO than for TMU. We specifically address the issue of the rotation-translation coupling. We then use a recently developed description of the role of the local environment on the hydrogen(H)-bond dynamics to relate the solution structure to the water dynamical properties in section 5. We end in section 6 with some concluding remarks.

2. SIMULATION METHODOLOGY

All molecular dynamics simulations presented within employ the water SPC-E model³⁹ and specific solute force fields for TMAO⁴⁰ and TMU.⁴¹ These solute force fields were shown to provide a description of aqueous solutions consistent with experimental data both at low and high solute concentrations.^{40,41} All simulation boxes contain a total of 500 molecules at the experimental density.^{42–44} We simulated a series of solutions with increasing solute molality, respectively, 0.1, 1, 2, 4, 6, and 8 mol/kg (m). For TMAO, these molalities correspond to concentrations of 0.1, 1, 1.8, 3.1, and 5.1 mol/L, and for TMU the successive concentrations are 0.1, 1, 1.7, 2.8, and 4.2 mol/L. For every solute concentration, the same procedure is followed with only a change in the solution density and therefore in the simulation box size. The system is first equilibrated in the canonical ensemble at $T = 298$ K for 100 ps. The trajectory is then propagated in the microcanonical ensemble for more than 1 ns, with a 1-fs time step and periodic boundary conditions, treating the long-range electrostatic interactions through Ewald summation. The resulting average temperature is 298 ± 1 K.

3. MICROSCOPIC STRUCTURE OF CONCENTRATED SOLUTIONS

While TMAO and TMU are structurally quite similar (Figure 1), both exhibiting a hydrophilic oxygen head and a hydrophobic moiety made respectively of three and four methyl groups, they behave very differently in concentrated aqueous solutions. On the one hand, TMU exhibits the usual behavior of hydrophobic solutes in aqueous solution and starts forming aggregates already at very low concentrations. Such clustering has been firmly established through small-angle neutron scattering (SANS),³⁷ thermodynamic data,³⁶ and NMR³⁵ measurements for concentrations as low as one TMU molecule for 100 water molecules (i.e., ≈ 0.5 m).⁴⁵ On the other hand, TMAO dissolves in water without aggregating up to very high concentrations^{38,40} (e.g., one TMAO for seven water molecules, i.e., ≈ 8 m), due to the strong electrostatic intermolecular interaction between the hydrophilic heads ($N^+ - O^-$), which counterbalances the attractive hydrophobic interaction. TMU and TMAO also have opposite effects on protein stability, TMU being a strong denaturing agent⁴⁶ while TMAO is a folding chaperone.⁴⁷

We now use our simulations to determine and contrast the microscopic structures of the two solutions as the concentration

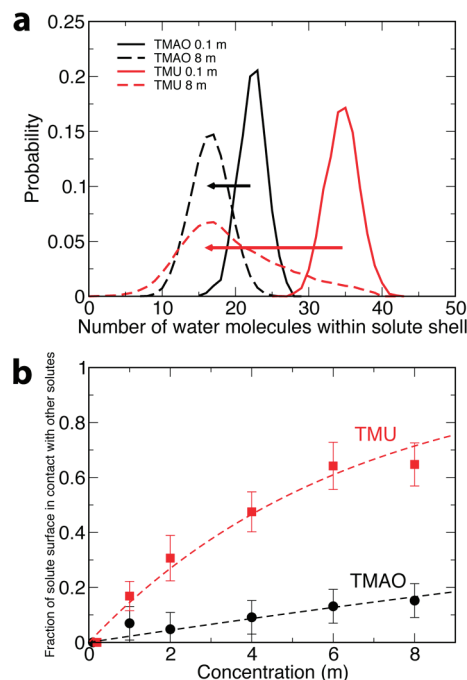


Figure 2. (a) Probability distributions of the number of water molecules within the hydration shells of TMAO and TMU at low (0.1 m) and high (8 m) concentration. The decrease between the average values is approximately 57% for TMU, versus approximately 27% for TMAO. (b) Fraction of the solute surface in contact with another solute for increasing concentration; the dotted lines are only guides for the eye.

is increased. The solute aggregation can be characterized in different, complementary ways, detailed below.

First, we focus on the overlap between solute hydration layers when the concentration is increased. For the two solutes, Figure 2a compares the distributions of the number of water molecules within the solute hydration shell for very dilute (0.1 m) and very concentrated (8 m) solutions. A water molecule is considered to belong to a solute hydration layer when its minimum distance to the solute atoms (excluding the hydrogens) is shorter than a certain cutoff. This cutoff distance is determined for each heavy atom as the location of the first minimum in the radial distribution function between this atom and the water oxygens, and is typically 3.5 Å. Figure 2a shows strikingly different behaviors for TMAO and TMU. While TMAO tends to preserve its entire hydration shell even at high concentration, the hydration number of TMU is drastically reduced with increasing concentration, and its distribution becomes significantly broader. While the TMU hydration number in dilute solutions is larger than that of TMAO because of the larger number of methyl groups, its decrease with increasing concentration is so pronounced that it becomes smaller than that of TMAO at high concentration (Figure 2a). Such strong concentration dependence of the TMU hydration number is due to the aggregation of TMU molecules, which protects methyl groups from a contact with water. Our results are consistent with prior studies^{38,48} based on simulations and near-infrared spectroscopy which had also evidenced the stability of the TMAO hydration layer with increasing concentration, in contrast to the pronounced decrease observed for another hydrophobic solute, *tert*-butyl alcohol, which behaves like TMU.

A complementary and original analysis of the solute distribution in the solution is provided by the relative aggregation surface

per solute molecule. This corresponds to the fraction of the solute surface that is in contact with another solute. It is computed by first performing a Voronoi tessellation of space:^{49,50} for each solute heavy atom and each solvent atom in the simulation box, its Voronoi polyhedra includes all the points closer to this atom than to any other (this is analogous to building Wigner–Seitz cells in a crystal). The surface of the solute molecule is the sum over all the solute atoms of the Voronoi polyhedra facet areas, excluding the facets shared between two atoms belonging to the same solute molecule. Figure 2b reports the fraction of this solute surface which is in contact with another solute. This fraction vanishes for infinitely dilute solutions and increases with concentration due to the aggregation of hydrophobic groups. Figure 2b shows that aggregation appears very rapidly for TMU, while the moderate increase observed for TMAO reflects the creation of a solute network within the solution but not a phase separation. The large aggregation observed for TMU, even at very low concentrations, is thus totally consistent with prior experiments³⁷ which had observed a non-negligible solute clustering beyond 0.5 m, but whose results have been ignored or misinterpreted in recent studies of water dynamics.^{24,25,27,28}

To directly connect our simulations to experiments which have probed the aggregation propensity of these solutes, we have also calculated the Kirkwood–Buff integral⁵¹ between TMU solutes. This integral is defined as $G_{\text{TMU-TMU}} = \int_0^\infty (g_{\text{TMU-TMU}}(r) - 1) \cdot 4\pi r^2 dr$, where $g_{\text{TMU-TMU}}(r)$ is the TMU–TMU radial distribution function. It measures the excess or deficiency of other solute molecules in the space around a given solute. Molecules that tend to cluster together lead to positive values of this integral. The values of the Kirkwood–Buff integral between TMU solutes computed from our simulations are clearly positive (e.g., at 1 m, $G_{\text{TMU-TMU}} \approx 400 \text{ cm}^3/\text{mol}$) and are quantitatively consistent with the experimental values³⁷ (at 1 m, $G_{\text{TMU-TMU}} \approx 410 \text{ cm}^3/\text{mol}$), which evidence the presence of a nonideal behavior due to aggregation.

These complementary studies therefore describe two very different microscopic structures and distributions of solute molecules for concentrated TMAO and TMU solutions, respectively. While TMAO molecules remain homogeneously distributed and retain their hydration layer up to very high concentrations, TMU molecules tend to segregate from water and form clusters.

4. WATER TRANSLATIONAL AND REORIENTATIONAL DYNAMICS

We now examine the impact of these two very different microscopic structures on the dynamics of water confined between these solute molecules. We successively focus on the translational and reorientational dynamics of water, before studying the coupling between these motions and its possible breakdown induced by a high solute concentration.

4.1. Translational Motion. Figure 3 shows the (translational) mean square displacement (MSD) of water for increasing TMU (Figure 3a) and TMAO (Figure 3b) concentrations, respectively. As the solute concentration increases, the water translational dynamics slows down with respect to the bulk. This slowdown is quantified by calculating the translational time τ_T as the time requested for a water molecule to cover a distance of 3 Å, a characteristic molecular length scale for liquid water (approximately the distance to the first shell), and defining the translational

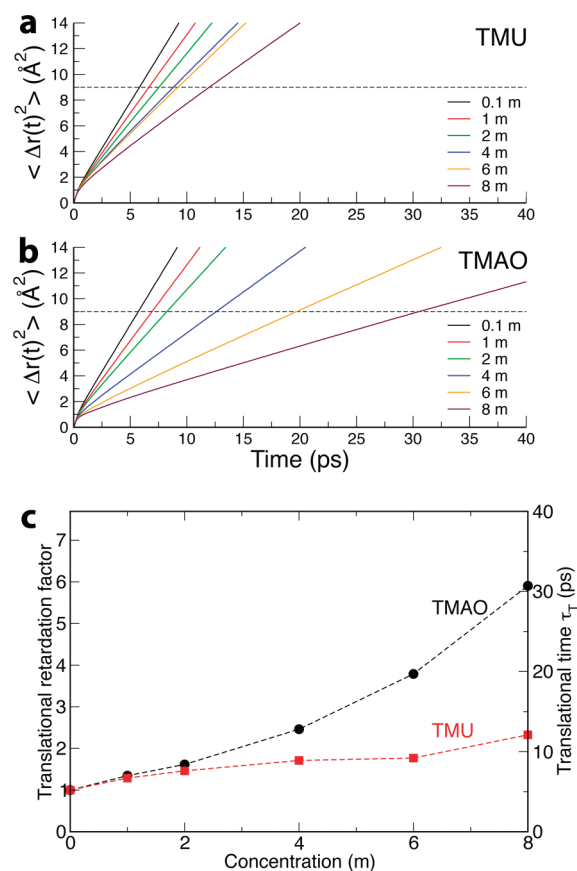


Figure 3. MSD for water molecules in (a) TMU and (b) TMAO aqueous solutions. The horizontal dashed line indicates the characteristic molecular distance used to define the translational time. (c) Characteristic translational time τ_T required for a water molecule to diffuse over a 3 Å distance in TMAO and TMU solutions, as a function of concentration, and its slowdown factor compared to the bulk value.

retardation factor with respect to the bulk as $\rho_T = \tau_T / \tau_T^{\text{bulk}}$, where the bulk time is $\tau_T^{\text{bulk}} \approx 5.2$ ps. Figure 3c shows that the water translational dynamics is always less retarded in TMU aqueous solutions than in TMAO solutions, and this difference increases with increasing concentration. In 8 m solutions, the retardation factor is $\rho_T \approx 2.3$ for TMU, while it is more than twice greater, $\rho_T \approx 5.8$, for TMAO solutions. We note that very similar results for the retardation factors can be obtained by computing the translational diffusion coefficient D , following Einstein's formulation, and performing a linear fit of the MSD at very long times. The extracted diffusion coefficients compare well with experimental data^{52,53} and previous simulations.⁴⁰

A closer examination of the water MSD (Figure 3) shows that a transient regime exists between the initial ballistic regime where the translational motion is inertial and the onset of the long-time translational diffusion regime where the MSD scales linearly with time. In this intermediate regime, the MSD scales sublinearly with time. This anomalous dynamics is best evidenced by plotting $\langle \Delta r(t)^2 \rangle / t$ along time on a log–log scale, as shown in Figure 4. Assuming a power-law dependence of the MSD with time, $\langle \Delta r(t)^2 \rangle \propto t^\alpha$, the slope of a linear fit on such a log–log representation yields the $\alpha - 1$ exponent. At long delays, when the diffusion regime is attained, $\langle \Delta r(t)^2 \rangle / t$ reaches a plateau value which is $6D$. Such subdiffusive dynamics are usually interpreted as originating from crowding effects,⁵⁴ here due to the presence

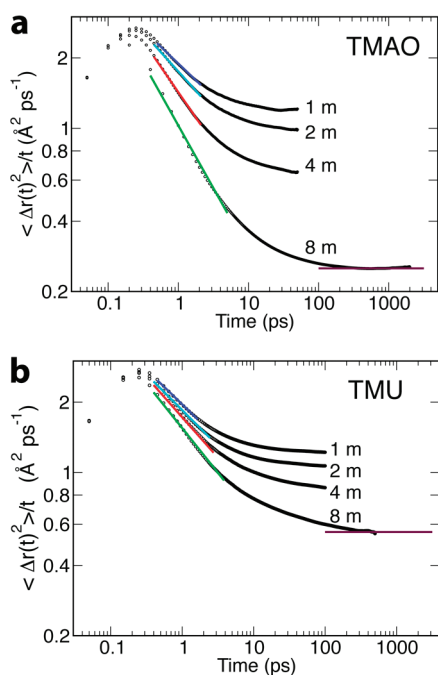


Figure 4. Log–log representation of $\langle \Delta r(t)^2 \rangle / t$ along time for (a) TMAO and (b) TMU aqueous solutions. Linear fits of the transient decay are used to extract the $(\alpha - 1)$ exponent. The horizontal asymptote signals the onset of the diffusive regime.

of many solute molecules, which locally hinder the water translational motions. Figure 4a shows that for TMAO solutions, the α exponent differs increasingly from 1 with increasing solute concentration ($\alpha = 0.71$ at 1 m vs $\alpha = 0.46$ at 8 m), and the onset of the diffusive regime becomes further delayed, reflecting the increased confinement due to the solute molecules. For TMU solutions (Figure 4.b), the sublinear character is less pronounced than for TMAO (at 8 m, $\alpha = 0.61$), thus suggesting a reduced confinement effect compared to TMAO. The microscopic origin of such anomalous dynamics will be discussed in detail in section 5.4.

4.2. Reorientational Motion. We now turn to the reorientational dynamics of water, and its dependence both on the solute nature and on the solute concentration.

We focus on the reorientation dynamics of the water OH bonds, which can be monitored through the time correlation function $c(t) = \langle P_2[\mathbf{u}_{\text{OH}}(0)\mathbf{u}_{\text{OH}}(t)] \rangle$, where P_2 is the second-order Legendre polynomial and $\mathbf{u}_{\text{OH}}(t)$ is the orientation of the water OH bond at time t .

In contrast to the bulk water case at room temperature where the decay of this orientation time correlation function is monoexponential past the initial librational regime (i.e., beyond approximately 200 fs),⁵⁵ in concentrated solutions of amphiphiles these decays exhibit a pronounced nonexponential behavior (Figure 5a). In order to characterize these relaxations, we therefore first rescale $c(t)$ to remove the librational drop and perform a time-integration of the decay to obtain the $\langle \tau_2 \rangle$ relaxation time. In the bulk case, this time-integrated relaxation time coincides with the long-time decay $\tau_2^{\text{bulk}} = 2.5$ ps.⁵⁵ The rotational retardation factor ρ_R is then defined as $\rho_R = \langle \tau_2 \rangle / \tau_2^{\text{bulk}}$ (We note that very similar results for ρ_R can be obtained by using a stretched exponential fit of $c(t)$).

The values of $\langle \tau_2 \rangle$ and ρ_R averaged over all water molecules are shown in Figure 5b for TMAO and TMU solutions of increasing concentration. Consistent with previous work,²⁹ the reorientation

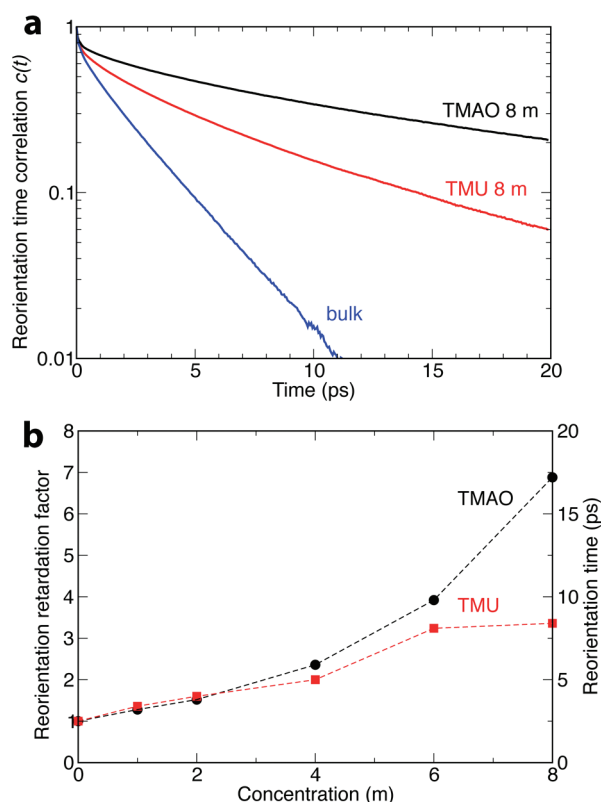


Figure 5. (a) Orientation time–correlation function $c(t)$ for 8 m TMAO and TMU aqueous solutions, together with the bulk reference. (b) Reorientation relaxation time $\langle \tau_2 \rangle$ and associated slowdown factor compared to the bulk for water molecules in TMAO and TMU solutions of increasing concentration.

time $\langle \tau_2 \rangle$ increases dramatically with increasing solute concentration. The slowdown factors calculated for TMU solutions are quantitatively consistent with NMR measurements⁵⁶ over the entire concentration range. We note that the reorientational dynamics is systematically more retarded in TMAO solutions than in TMU solutions, similarly to what was observed for the translational dynamics in section 4.1.

4.3. Rotation–Translation Coupling. We now focus on the coupling between translational and rotational water dynamics. For bulk liquid water, such coupling can be expected from the experimentally observed parallel evolution with temperature of dynamical quantities pertaining to translation (e.g., translational diffusion constant) and to the reorientation (e.g., reorientation time).⁵⁷ Such coupling is usually discussed within the Debye–Stokes–Einstein model, which relates translational and reorientational dynamics. However, for water reorientation, the Debye diffusion model is not valid,^{55,58} and a large-amplitude jump reorientation mechanism has recently been suggested.^{55,58} Within this new model, rotation and translation motions are still intimately coupled because reorientation results from exchanges of H-bond acceptors, which involve translational motions for the departure of the old partner and the arrival of the new one. However, in some situations, the rotation–translation coupling has been suggested to breakdown, for example, at low temperature in supercooled water,⁵⁹ in the vicinity of sugars,⁶⁰ and in concentrated polymer aqueous solutions (e.g., poly(ethylene oxide)).⁶¹ Such a decoupling is usually ascribed to the presence of dynamical heterogeneities.⁵⁹

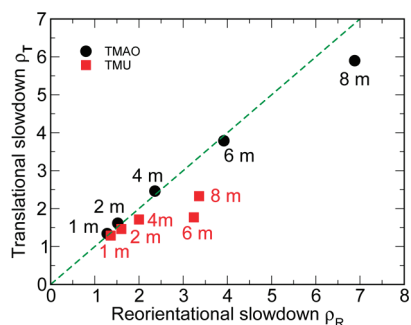


Figure 6. Correlation between reorientational ρ_R and translational ρ_T retardation factors for water dynamics in increasingly concentrated TMAO and TMU aqueous solutions.

The possible presence of a decoupling between the translational and reorientational water motions in concentrated solutions is of great importance for the understanding of water dynamics in the cell cytoplasm. For the dynamics of water in the cellular media of an extreme halophilic archaeon, QENS experiments²² have measured translational dynamics 250 times slower than in the bulk, while NMR²³ has measured rotational dynamics only 15 times slower than in the bulk. These conflicting experimental results could possibly be reconciled if the translational and rotational dynamics of water became decoupled because of the large solute concentration in the cytoplasm.

The translational and rotational retardation factors for water in TMAO and TMU solutions are shown in Figure 6. The translational and rotational dynamics are surprisingly closely correlated up to very high concentrations. We only observe a weak decoupling at 8 m for TMAO and above 6 m for TMU. In both cases, the rotational dynamics is more slowed down than the translational dynamics (at 8 m, $\rho_R/\rho_T = 1.14$ for TMAO and 1.25 for TMU). While TMU and TMAO are obviously not representative of all types of solutes that can be found in the cytoplasm, we note that the range of concentrations we have studied covers the typical cytoplasm conditions, and that the reorientational slowdown factors found in the simulations have the same order of magnitude as those found by NMR. Our results thus do not support the hypothesis of a decoupling between translational and reorientational motions to explain the discrepancy between the NMR and QENS measurements.

Our results also show that while both TMAO and TMU retard the translational and reorientational dynamics of water for increasing solute concentrations, their respective effects on the dynamics of water are very different, TMAO being a much more potent retardant.

5. RELATIONSHIP BETWEEN LOCAL STRUCTURE AND WATER DYNAMICS

In order to relate the water dynamics to the microscopic structure of the aqueous solution, we will extend the ideas we have recently developed to describe how the water H-bond dynamics is affected by the local environment. For a water molecule in solution, the breaking of a H-bond with an initial partner and the forming of a H-bond with a new partner are necessary both for reorientations leading to a new stable orientation and for translational displacements ending in a new stable position. The study of H-bond dynamics will thus provide a common ground to determine the influence of the local

environment. This will lead to a connection between the local structure and the water dynamics which will be used to rationalize why the different TMU and TMAO solute distributions result in very different water dynamics.

5.1. Extended Jump Model. It was recently suggested that beyond an initial <200 fs period where a water OH group librates around its H-bond axis, the OH reorientation proceeds along two independent pathways.^{55,58,62} The most important route is via the exchange of H-bond acceptors, where once the environment has reorganized to offer a new viable H-bond acceptor, the water OH bond suddenly executes a large amplitude angular jump from its former H-bond partner to this new acceptor.^{55,58,62} An additional minor contribution to the reorientation is through the diffusive tumbling of the intact H-bond axis between successive jumps.^{55,58,62} This extended jump model has then been successfully applied to a broad range of situations, including, e.g., ionic solutions,⁶³ aqueous solutions of amphiphilic solutes including TMAO and TMU,^{29,64} solutions of amino acids,⁶⁵ and the vicinity of an extended hydrophobic interface.⁶⁶

In a previous work,²⁹ some of us already showed that the measured retardation of the reorientation time in TMAO and TMU solutions is caused by a slowdown in both the H-bond exchanges and the frame tumbling between successive jumps. The slowdown in the H-bond exchange time was shown to originate from an excluded-volume effect at the jump transition state, due to the presence of solutes. The presence of hydrophobic groups hinders the approach of some new water H-bond acceptors, thus slowing down the exchange rate. This transition-state excluded volume (TSEV) effect leads to the ρ_V retardation factor, which is determined from the fraction f of transition state locations for the new partner, which are forbidden by the presence of solute molecules, $\rho_V = 1/(1 - f)$.²⁹ When the concentration of hydrophobic groups increases, the fraction f increases, and the slowdown factor ρ_V increases. For water molecules donating an H-bond to a solute acceptor site, an additional effect originating from the transition-state hydrogen bond (TSHB) strength was also shown to be important, especially for very strong H-bond acceptor groups,^{64,65} and the overall slowdown in the H-bond exchange dynamics was expressed as the product of the two factors $\rho = \rho_V \rho_{HB}$.

5.2. Local Environment and Slowdown Factor Distribution. The TSEV effect has already been shown to quantitatively predict the reorientational slowdown factors for dilute TMAO and TMU solutions and over a broad concentration range for TMAO solutions.²⁹ We extend here this previous approach and apply the TSEV model to understand the origin of the different impacts of TMAO and TMU on water when in concentrated solutions.

Figure 7 shows the distribution of slowdown factors ρ for the 8 m TMAO and TMU solutions, including both the TSEV and TSHB factors. With respect to our previous work which had exclusively focused on the water molecules residing next to hydrophobic groups,²⁹ we now include all waters in the solution. The TSHB effect for water molecules donating H-bonds to the TMAO solute hydrophilic heads enhances the distribution at large retardation factor values. The TMAO and TMU distributions are dramatically different. The TMU distribution exhibits two peaks: one narrow peak corresponding to bulk-like dynamics ($\rho = 1$) and a broad band whose maximum lies at $\rho = 1.5$, i.e., the typical slowdown value measured for water next to a single hydrophobic solute. In contrast, the TMAO distribution exhibits a single, very broad peak, which extends to much larger ρ values.

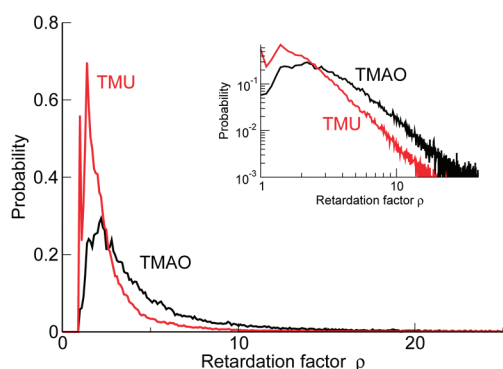


Figure 7. Distributions of the H-bond exchange retardation factor ρ compared to the bulk for 8 m TMAO and TMU solutions. ρ is calculated through the TSEV/TSHB model and is the product of the TSEV (ρ_V) and transition-state H-bond strength (ρ_{HB}) factors. The same distributions are represented in the inset on a log–log scale, which evidences their power law tails.

These two distributions reflect the very different local environments experienced by water molecules in the two solutions. Additional insight is provided by the calculation of the fraction of interfacial solvent atoms lying next to a solute molecule for increasing TMU and TMAO concentrations (Figure 8a). A solvent atom is defined as interfacial if it shares at least one Voronoi polyhedra facet with a solute atom.

Figure 8a shows that for increasing TMAO concentrations, the organization of the solute molecules strongly confine the water solvent, bulk water disappears, and almost all the water molecules ($\approx 94\%$ at 8 m) become interfacial. At high concentration, water molecules form thin films and narrow wires, which percolate through the solution (Figure 8b) (We verified that the water network is above the percolation threshold by computing the size of the largest cluster of H-bonded water molecules formed in the solution). The very broad single-peak distribution of slowdown factors where all waters are retarded compared to the bulk, which has been calculated for the 8 m TMAO solution (Figure 7) can thus be explained by the local environment of these water molecules: they are all interfacial, and thus all slowed down, and the width of the distribution originates from the variety of local environments that can be experienced by a water molecule.

In contrast, for TMU aqueous solutions, Figure 8a shows that even at the highest concentration examined in our study (8 m), a non-negligible fraction of the solvent ($\approx 15\%$) is not in direct contact with the solutes. These molecules are in the middle of water subnanometer pools which form as a result of TMU segregation (Figure 8b).⁶⁷ These water molecules therefore exhibit bulk-like dynamics and explain the presence of the first peak with no retardation ($\rho = 1$) in the distribution of slowdown factors (Figure 7). The other water molecules lie at the interface with a TMU solute, but most of them are next to a single solute at a time, in contrast to the TMAO solution where a water molecule can be surrounded by several solute molecules simultaneously. This explains why the slowdown factors appearing in the TMU distribution (Figure 7) are similar to those found next to a single dilute hydrophobic solute.

We also note that Figure 8a clearly shows that the number of interfacial water molecules scales extremely nonlinearly with the solute concentration, even at low concentration. This shows that the linear scaling approximation used to interpret a recent series of experiments^{24,25,28} should be revised.

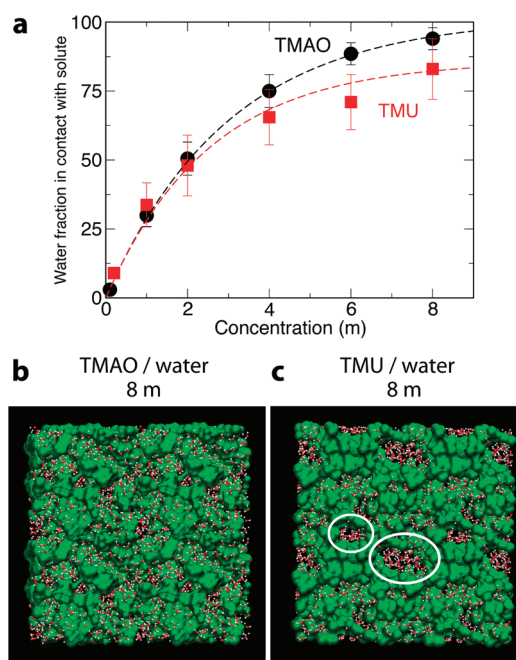


Figure 8. (a) Fraction of interfacial water molecules among all the water molecules in the solution. Representative snapshots of the (b) TMAO and (c) TMU binary solutions at $c = 8$ m, with the solute molecules displayed in green. For clarity, the simulation cell is represented along one of its images along the x and y directions. The locations of some water subnanopools resulting from TMU aggregation are highlighted.⁶⁷

5.3. Impact on Reorientation Dynamics. We now examine how the very different microscopic environments experienced by water molecules in concentrated TMAO and TMU solutions and the ensuing different distributions of slowdown factors can rationalize the different water dynamics we measured in these two solutions. We first consider the reorientation dynamics, which as explained above is due to H-bond exchanges and to the tumbling of intact H-bond axes between exchanges.

The slowdown in the H-bond exchange time induced by TMU and TMAO has already been presented in ref 29 for the water molecules lying next to a hydrophobic group. We present here the average exchange time for all the water molecules in the solution, thus including the water molecules donating a H-bond next to a solute acceptor site or lying in a water subnanopool. The deviation between the H-bond exchange times measured in concentrated TMAO and TMU solutions reflect very well the very different distributions presented above for the slowdown factors. In the 8 m TMAO solution, the directly computed slowdown factor is 3.7 (Figure 9), in perfect agreement with the 3.7 average value from the ρ distribution determined via the TSEV/TSHB model (Figure 7), and in the 8 m TMU solution, the directly computed slowdown is 2.5 (Figure 9), in excellent agreement with the 2.4 average value from the TSEV/TSHB model distribution (Figure 7). The greater slowdown observed for concentrated TMAO solutions compared to TMU solutions is due to the microscopic structure of the solution, where, as explained above, no water molecule remains bulk-like, and many water molecules are surrounded by several TMAO molecules, thus leading to large excluded volume fractions f and large slowdown factors.

We pause to note here that the agreement between the slowdown factors predicted by our extended jump model and

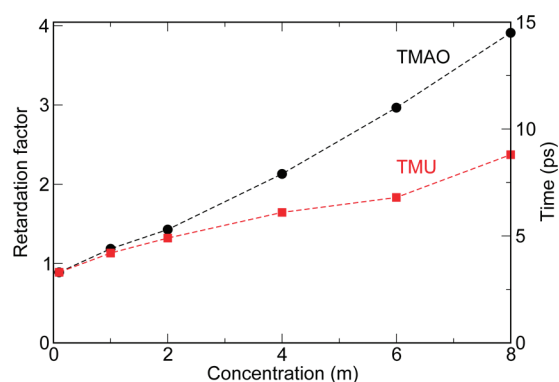


Figure 9. H-bond jump exchange times for water molecules in increasingly concentrated TMAO and TMU aqueous solutions.

directly calculated in the simulations is surprisingly good. Our model indeed only includes local effects through the TSEV and TSHB factors, describing the local influence of an interface on the water dynamics. In extreme confinement situations, additional nonlocal effects are expected, since the interface is no longer in contact with bulk water, but with a more structured water due to the slowly relaxing confining geometry. The free energy cost for the approach of the new water partner is thus expected to increase compared to the bulk situation, further retarding the water dynamics.

We have also considered the minor contribution to the overall reorientation due to the tumbling of an intact H-bond.^{55,58,62} Increasing the solute concentration slows down this motion considerably, but does so very differently for the two solutes. In 8 m solutions, this reorientation is retarded by a factor 14 for TMAO and only 3 for TMU. Such results are consistent with the measured increase in the solution viscosity with increasing solute concentration, which is much more pronounced for TMAO⁶⁸ than for TMU.⁶⁹

5.4. Microscopic Origin of the Subdiffusive Translational Dynamics. We now turn to the study of the impact of the local structure on the short-time translational dynamics.

We showed in section 4.1 that the translational dynamics of water exhibits an anomalous subdiffusive regime, which is increasingly pronounced for increasing solute concentration, especially for TMAO (Figure 4). Two different models are usually invoked to explain subdiffusive dynamics. The first model describes the translational displacement as a continuous time random walk (CTRW) process,^{70,71} i.e., a Brownian diffusion model with a distribution of waiting times between two consecutive steps following a power law $\psi(\tau) \sim \tau^{-\nu}$. Such distribution leads to subdiffusive dynamics when $0 < \nu < 2$.⁷⁰ The CTRW model was, for example, invoked to explain the observed anomalous dynamics of water confined in complex environments such as protein interfaces.^{72,73} The second possibility to explain the presence of subdiffusive dynamics is a change in the dimensions of the space explored by translation. It has been shown that a random walk occurring in a fractal space can also lead to a subdiffusive behavior.⁷⁴

We thus explored these two possibilities, which can be summarized as either an energetic disorder (CTRW model) or a topological disorder (fractal space model), in the case of concentrated TMU and TMAO solutions. The distribution of waiting times in the CTRW model can be reasonably approximated by the distribution of slowdown factors for the H-bond

exchanges, since we just showed that rotation and translation remain well coupled even at high concentration. This distribution has been computed for 8 m solutions of TMU and TMAO and exhibits a tail for large slowdown factors, which follows a power law $\rho^{-\nu}$ (see Figure 7 inset), whose exponent is, respectively, $\nu = 2.3$ and $\nu = 3.0$ for TMAO and TMU aqueous solutions. Since in both cases $\nu > 2$, this implies that such distributions are not sufficiently broad to explain the subdiffusive dynamics within the CTRW model.

Regarding the dimension of the space accessible to water in such concentrated solutions, we estimated via a block-counting algorithm that for 8 m TMAO, the water molecules no longer diffuse in a regular three-dimensional space but rather in a geometry whose fractal dimension is $d_f = 2.39$ (in a space of fractal dimension d_f the number of particles within a sphere of radius r scales as r^{d_f}). Since for a three-dimensional network there is no rigorous relationship between the fractal dimension and the subdiffusive exponent α for the MSD $\langle \Delta r(t)^2 \rangle \propto t^\alpha$,⁷⁴ we can only qualitatively suggest that the topological disorder may explain the subdiffusive dynamics.

However, the importance of the topological disorder in such concentrated solutions does not imply that the energetic disorder does not play any role. Following a strategy successfully used to investigate the dynamics of water next to proteins⁷⁵ and in carbohydrate solutions,²⁰ we considered an 8 m TMAO solution where all the solute molecules are kept frozen, thus ensuring that the geometry explored by the water molecules is unchanged. We then compared two simulations: one where the full interactions between water and solute molecules are considered (i.e., including both the electrostatic and van der Waals terms) and another one where the electrostatic term is removed. The water translational times τ_T (defined in section 4.1) are 30 ps for the regular system, 127 ps for the frozen solutes with their full charges, and 39 ps for the frozen solutes with no electrostatic charges (a similar trend has been observed in the case of proteins⁷⁵ and carbohydrate solutions²⁰). The subdiffusive regime is thus affected by the electrostatic interaction term, which shows that the energetic disorder plays a non-negligible role, even if it cannot explain the subdiffusive dynamics by itself.

6. CONCLUDING REMARKS

In this contribution, we have investigated how the reorientation and translation dynamics of water are affected by the presence of an increasing concentration of amphiphilic solutes. We first evidenced the dramatic slowdown in the water dynamics with increasing solute concentration, which is quantitatively described by the increasing excluded volume fraction occupied by the solute molecules. The large slowdown observed at high concentrations of amphiphiles is not an intrinsic effect of these solutes (e.g., a hydrophobic effect) but rather stems from the confinement caused by the very high solute density. This further demonstrates that experiments performed on concentrated solutions^{24–28} cannot be used to infer the dynamical behavior of water next to dilute solutes.

By contrasting two amphiphilic solutes, TMAO and TMU, we also evidenced that the aggregation properties of the solute at high concentration determine the microscopic distribution of solute molecules throughout the solution, which has a critical impact on the distribution of excluded volume factors and thus on the water dynamics. For solutes such as TMU that aggregate readily, water molecules tend to be segregated into small pools;

the water dynamics in the core of these pools is bulk-like, while the dynamics at the interface is moderately slowed down, resembling the situation next to a dilute hydrophobic group. In contrast, for concentrated nonaggregating solutes such as TMAO, water molecules form a thin film between the solute molecules, and they are all surrounded by more than one solute, leading to much more pronounced dynamical slowdowns. While we showed in a previous study that in dilute solutions, different hydrophobic groups induce very similar and moderate slowdowns for the water reorientation dynamics, we find here that in concentrated solutions, the reorientational and translational dynamics of water are critically sensitive to the type of hydrophobic solute and especially to its aggregation propensity.

Our study thus calls for a careful reinterpretation of the recent series of experiments performed on concentrated TMU aqueous solutions,^{24–28} and which ignored several critical points. First, the slowdown magnitude induced by hydrophobic groups is strongly concentration-dependent. Second, beyond the aggregation threshold (as low as 0.5 m for TMU), the number of water molecules affected by the solutes does not scale linearly with the solute concentration. The ill-characterized temperature dependence of aggregation also precludes any straightforward analysis of the temperature-dependence of water dynamics.²⁸ Our results eventually evidence that translational and reorientational dynamics remain significantly coupled even at very high solute concentrations, thus suggesting that the discrepancy observed between recent QENS and NMR measurements for water dynamics in cellular media may not be justifiable by such a decoupling.

AUTHOR INFORMATION

Corresponding Author

*E-mail: fabio.sterpone@ibpc.fr (F.S.); damien.laage@ens.fr (D.L.).

Present Addresses

[†]Laboratoire de Biochimie Théorique, UPR9080 CNRS, Institut de Biologie Physico-Chimique, 13 rue Pierre et Marie Curie, 75005 Paris, France.

Author Contributions

[†]These authors contributed equally to this work.

ACKNOWLEDGMENT

We thank the P. G. de Gennes Foundation for Research (Paris) for a postdoctoral fellowship to F.S., and CASPUR (Rome) for a generous allocation of computational resources (STD09-366).

REFERENCES

- (1) Rashin, A. A.; Iofin, M.; Honig, B. *Biochemistry* **1986**, *25*, 3619–3625.
- (2) Ball, P. *Chem. Rev.* **2008**, *108*, 74–108.
- (3) Bernèche, S.; Roux, B. *Nature* **2001**, *414*, 73–77.
- (4) Persson, E.; Halle, B. *J. Am. Chem. Soc.* **2008**, *130*, 1174–1187.
- (5) Malikova, N.; Cadène, A.; Marry, V.; Dubois, E.; Turq, P. *J. Phys. Chem. B* **2006**, *110*, 3206–3214.
- (6) Moilanen, D. E.; Piletic, I. R.; Fayer, M. D. *J. Phys. Chem. C* **2007**, *111*, 8884–8891.
- (7) Faeder, J.; Ladanyi, B. M. *J. Phys. Chem. B* **2000**, *104*, 1033–1046.
- (8) Abel, S.; Sterpone, F.; Badyopadhyay, S.; Marchi, M. *J. Phys. Chem. B* **2004**, *108*, 19458–19466.

- (9) Dokter, A.; Wourtersen, S.; Bakker, H. J. *Proc. Natl. Acad. Sci. U.S.A.* **2006**, *103*, 15355–15358.
- (10) Moilanen, D. E.; Fenn, E. E.; Wong, D.; Fayer, M. D. *J. Chem. Phys.* **2009**, *131*, 014704.
- (11) Levinger, N. E.; Swafford, L. A. *Annu. Rev. Phys. Chem.* **2009**, *60*, 385–406.
- (12) Rasaiah, J. C.; Garde, S.; Hummer, G. *Annu. Rev. Phys. Chem.* **2008**, *59*, 713–740.
- (13) Koga, K.; Tao, G. T.; Tanaka, H.; Zeng, X. C. *Nature* **2001**, *412*, 802–805.
- (14) Ricci, M. A.; Bruni, F.; Gallo, P.; Rovere, M.; Soper, A. K. *J. Phys.: Condens. Matter* **2000**, *12*, A345–A350.
- (15) Caille, F.; Stirnemann, G.; Boutin, A.; Demachy, I.; Fuchs, A. H. *J. Phys. Chem. C* **2008**, *112*, 10435–10445.
- (16) Giovambattista, N.; Rossky, P. J.; Debenedetti, P. *Phys. Rev. E* **2006**, *73*, 041604.
- (17) M. Sharma, E. S.; Donadio, D.; Galli, G. *Nano Lett.* **2008**, *8*, 2959–2962.
- (18) Fayer, M. D.; Levinger, N. E. *Annu. Rev. Anal. Chem.* **2010**, *3*, 89–107.
- (19) Bellissent-Funel, M.-C. *Eur. Phys. J. E* **2003**, *12*, 83–92.
- (20) Pomata, M. H. H.; Sonoda, M. T.; Skaf, M. S.; Elola, M. D. *J. Phys. Chem. B* **2009**, *113*, 12999–13006.
- (21) Ellis, R. J.; Minton, A. P. *Nature* **2003**, *425*, 27–28.
- (22) Frölich, A.; Gabel, F.; Jasmin, M.; Lehnert, U.; Oesterheld, D.; Tehei, A. M.; Weik, M.; Wood, K.; Zaccai, G. *Faraday Discuss.* **2009**, *141*, 117–130.
- (23) Qvist, J.; Persson, E.; Mattea, C.; Halle, B. *Faraday Discuss.* **2009**, *141*, 131–144.
- (24) Rezus, Y. L. A.; Bakker, J. H. *Phys. Rev. Lett.* **2007**, *99*, 148301.
- (25) Petersen, C.; Tielrooij, K.-J.; Bakker, J. H. *J. Chem. Phys.* **2009**, *130*, 214511.
- (26) Bakulin, A. A.; Linag, C.; Jansen, T. L. C.; Wiersma, D. A.; Bakker, H. J.; Pshenichnikov, M. S. *Acc. Chem. Res.* **2009**, *42*, 1229–1238.
- (27) Bonn, M.; Bakker, H. J.; Rago, G.; Pouzy, F.; Siekierzycka, J. R.; Brouwer, A. M.; Bonn, D. *J. Am. Chem. Soc.* **2009**, *131*, 17070–17071.
- (28) Tielrooij, K. J.; Hunger, J.; Buchner, R.; Bonn, M.; Bakker, H. J. *J. Am. Chem. Soc.* **2010**, *132*, 15671–15678.
- (29) Laage, D.; Stirnemann, G.; Hynes, J. T. *J. Phys. Chem. B* **2009**, *113*, 2428–2435.
- (30) Heisler, I. A.; Meech, S. R. *Science* **2010**, *327*, 857–860.
- (31) Mazur, K.; Heisler, I. A.; Meech, S. R. *J. Phys. Chem. B* **2010**, *114*, 10684–10691.
- (32) Lupi, L.; Comez, L.; Masciovecchio, C.; Morresi, A.; Paolantoni, M.; Sassi, P.; Scarponi, F.; Fioretto, D. *J. Chem. Phys.* **2011**, *134*, 055104.
- (33) Qvist, J.; Halle, B. *J. Am. Chem. Soc.* **2008**, *130*, 10345–10353.
- (34) Silvestrelli, P. *J. Phys. Chem. B* **2009**, *113*, 10728–10731.
- (35) Holz, M.; Grunder, R.; Sacco, A.; Meleleo, A. *J. Chem. Soc. Faraday Trans.* **1993**, *89*, 1215–1222.
- (36) Marcus, Y. *Phys. Chem. Chem. Phys.* **2002**, *4*, 4462–4471.
- (37) Almásy, L.; Len, A.; Székely, N.; Pleštil, J. *Fluid Phase Equilib.* **2007**, *257*, 114–119.
- (38) Fornili, A.; Civera, M.; Sironi, M.; Fornili, S. L. *Phys. Chem. Chem. Phys.* **2003**, *5*, 4905–4910.
- (39) Straasma, T. P.; Berendsen, H. J. C.; Postma, J. P. M. *J. Chem. Phys.* **1986**, *85*, 6720.
- (40) Paul, S.; Patey, G. *J. Phys. Chem. B* **2006**, *110*, 10514–10518.
- (41) Bellatato, P.; Freitas, L. C. G.; Areas, E. P. G.; Santos, P. S. *Phys. Chem. Chem. Phys.* **1999**, *1*, 4769–4776.
- (42) Patil, K. J.; Sargar, A. M.; Dagade, D. H. *Indian J. Chem. A: Inorg., Bio-inorg., Phys., Theor. Anal. Chem.* **2002**, *41*, 1804–1811.
- (43) Kast, K. M.; Brickmann, J.; Kast, S. M.; Berry, R. S. *J. Phys. Chem. A* **2003**, *107*, 5342–5351.
- (44) Zou, Q.; Bennion, B. J.; Daggett, V.; Murphy, K. P. *J. Am. Chem. Soc.* **2002**, *124*, 1192–1202.
- (45) A similar clustering at very low concentration has been observed for other amphiphilic solutes, including, e.g., tertbutyl alcohol.⁶⁸

- (46) Pace, C. N.; Marshall, H. F. *Arch. Biochem. Biophys.* **1980**, *190*, 270–276.
- (47) Baskakov, I.; Bolen, D. W. *J. Biol. Chem.* **1998**, *273*, 4831–4834.
- (48) Michele, A. D.; Mariangela, F.; Onori, G.; Santucci, A. *J. Phys. Chem. A* **2004**, *108*, 6145–6150.
- (49) Voronoi, G. F. *J. Reine Angew. Math.* **1908**, *134*, 198–287.
- (50) Bernal, J. D.; Finney, J. L. *Discuss. Faraday Soc.* **1967**, *143*, 62–69.
- (51) Kirkwood, J. G.; Buff, F. P. *J. Chem. Phys.* **1951**, *19*, 774–777.
- (52) Cser, L.; Grész, T.; Jancsó, G.; Káli, G. *Physica B* **1997**, *234–236*, 4349–4350.
- (53) Hovagimyan, K. G.; Gerig, J. T. *J. Phys. Chem. B* **2005**, *109*, 24142–24151.
- (54) Saxton, M. J. *Biophys. J.* **2007**, *92*, 1178–1191.
- (55) Laage, D.; Hynes, J. T. *J. Phys. Chem. B* **2008**, *112*, 14230–14242.
- (56) Shimizu, A.; Fumino, K.; Yukiyasu, K.; Taniguchi, Y. *J. Mol. Liq.* **2000**, *85*, 269–278.
- (57) Chen, S. H.; Teixeira, J. *Adv. Chem. Phys.* **1986**, *64*, 1–44.
- (58) Laage, D.; Hynes, J. T. *Science* **2006**, *311*, 832–835.
- (59) Mazza, M. G.; Giovambattista, N.; Stanley, H. E.; Starr, F. W. *Phys. Rev. E* **2007**, *76*, 031203.
- (60) Lawrence, S.; Debenedetti, P. G.; Errington, J. R. *J. Chem. Phys.* **2005**, *122*, 204511.
- (61) Borodin, O.; Bedrov, D.; Smith, G. J. *J. Phys. Chem. B* **2002**, *106*, 5194–5199.
- (62) Laage, D.; Stirnemann, G.; Sterpone, F.; Rey, R.; Hynes, J. T. *Annu. Rev. Phys. Chem.* **2011**, *62*, 395–416.
- (63) Laage, D.; Hynes, J. T. *Proc. Natl. Acad. Sci. U.S.A.* **2007**, *104*, 11167–11172.
- (64) Stirnemann, G.; Hynes, J. T.; Laage, D. *J. Phys. Chem. B* **2010**, *114*, 3052–3059.
- (65) Sterpone, F.; Stirnemann, G.; Hynes, J. T.; Laage, D. *J. Phys. Chem. B* **2010**, *114*, 2083–2089.
- (66) Stirnemann, G.; Rossky, P. J.; Hynes, J. T.; Laage, D. *Faraday Discuss.* **2010**, *146*, 263–281.
- (67) Because of the strong segregation observed in TMU aqueous solutions, we cannot exclude that simulations on larger cells would lead to larger water pools.
- (68) Sinibaldi, R.; Casieri, C.; Melchionna, S.; Onori, G.; Segre, A. L.; Viel, S.; Mannina, L.; Luca, F. D. *J. Phys. Chem. B* **2006**, *110*, 8885–8892.
- (69) Okpala, C.; Guiseppi-Elie, A.; Maharajh, D. M. *J. Chem. Eng. Data* **1980**, *25*, 384–386.
- (70) Metzler, R.; Klafter, J. *Phys. Rep.* **2000**, *339*, 1–77.
- (71) Condamin, S.; Tejedor, V.; Voituriez, R.; Bénichou, O.; Klafter, J. *Proc. Natl. Acad. Sci. U.S.A.* **2008**, *105*, 5675–5680.
- (72) Bizzarri, A. R.; Cannistraro, S. *J. Phys. Chem. B* **2002**, *106*, 6617–6633.
- (73) Gallo, P.; Rovere, M. *J. Phys.: Condens. Matter* **2003**, *15*, 7625–7633.
- (74) ben Avraham, D.; Havlin, S. *Diffusion and Reactions in Fractals and Disordered Systems*; Cambridge University Press: Cambridge, U.K., 2000.
- (75) Pizzitutti, F.; Marchi, M.; Sterpone, F.; Rossky, P. *J. Phys. Chem. B* **2007**, *111*, 7584–7590.